Proceedings of the 25th International Conference on
Port and Ocean Engineering under Arctic Conditions
June 9-13, 2019, Delft, The Netherlands

Peridynamic modelling of polycrystalline ice

Wei Lu[1,2], Mingyang Li[1], Bozo Vazic[1], Selda Oterkus[1] and Erkan Oterkus[1]
[1]University of Strathclyde, Glasgow, UK
[2]Harbin Engineering University, Harbin, China

ABSTRACT

Due to the harsh environment of the Arctic region, ship structures must be designed to withstand ice loads in case of a collision between a ship and ice takes place. Although experimental studies can give invaluable information about ship-ice interactions, full scale tests are very costly to perform. Therefore, computer simulations can be a good alternative. Ice-structure interaction modelling is a very challenging process. First of all, ice material response depends on many different factors including applied-stress, strain-rate, temperature, grain-size, salinity, porosity and confining pressure. Furthermore, macro-scale modeling may not be sufficient to capture the full physical behaviour because the micro-scale effects may have a significant effect on macroscopic material behaviour. Hence, it is necessary to utilize a multi-scale methodology. By taking into account all these challenging issues, a state-of-the-art technique, peridynamics can be utilized for ice fracture modelling. Peridynamics is a non-classical (non-local) continuum mechanics formulation which is very suitable for failure analysis of materials due its mathematical structure. Cracks can occur naturally in the formulation and there is no need to impose an external crack growth law. Furthermore, due to its non-local character, it can capture the phenomenon at multiple scales. In this study, the utilization of peridynamics will be presented to simulate mechanical behaviour of polycrystalline ice by modelling individual grains.

KEY WORDS Peridynamics; Polycrystalline ice; Anisotropy; Numerical.

INTRODUCTION

In Arctic regions, the accurate prediction of ice behaviour plays a significant role in the optimum design of marine structures and polar ships. The naturally generated ice has usually polycrystalline structure which can be characterized by its average grain size, grain morphology, and grain orientation, and is highly dependent on the properties of grain boundary which can be been associated with microcracks (Gold 1960; Gold 1967; Gold 1999). Therefore, it is a great challenge to fully understand the behaviour of polycrystalline ice.

In order to study the behaviour of polycrystalline material, various experiments have been done by using X-ray analysis (Liu et al., 1992; Gay et al., 1954). However, although the results obtained from experiments provide very useful information for the future studies, the expensive cost of equipment and time-consuming procedures of preparation of the material limit its wide application. Currently, with the development of high-performance computing, the numerical simulations become one of the predominant approaches utilized in the polycrystalline material analysis. Amongst the computational techniques, the cohesive zone model (CZM) within the framework of the FEM method is one of the most widely used approaches for fracture analysis of polycrystalline systems. A two-dimensional finite element model was developed by Warner and Molinari (2006) to investigate intergranular fracture in alumina with the grain interiors modeled as anisotropic elastic material and the grain boundary properties were fitted with experimental data. Sfantos and Aliabadi (2007) proposed boundary cohesive grain element model to simulate the intergranular microfracture of SiC. To investigate the transition from an intergranular to a transgranular mode of fracture, the extended finite element method (XFEM) was used to model quasi-static crack propagation (Sukumar et al., 2003). For the polycrystalline ice, Gribanov et al. (2018) implemented the cohesive zone model within an implicit finite element method to simulate the 4-point bending test of freshwater ice beam. Although all these approaches provide useful information, since they are based on classical continuum mechanics, they inherit certain disadvantages of classical continuum mechanics (Crocker et al., 2005). Specifically, the governing equations of the classical continuum mechanics incorporate spatial displacement derivatives which are undefined along the crack surfaces and the interfaces where the displacement field is discontinuous. By taking these difficulties into consideration, a non-local meshfree method proposed by Silling (2000), called peridynamics, can be utilized for the simulation of the polycrystalline ice. In this formulation, integral equations are used instead of the partial differential equations. Therefore, it is suitable for predicting crack initiation and propagation which may occur spontaneously. Askari et al. (2008) and De Meo et al. (2016) simulated polycrystalline fracture in silicon and AISI 4340 steel, respectively, by using peridynamics for cubic crystal systems. Furthermore, Ghajari et al. (2014) presented a bond-based peridynamic formulation suitable for hexagonal crystal systems.

In this paper, the polycrystalline ice model for static analysis is proposed within the framework of the bond-based peridynamic theory. The peridynamic parameters are obtained by equating the strain energy density of a material point with the classical continuum mechanics. The numerical results of the simulation are compared with the results obtained from FEM to testify the accuracy of the numerical peridynamic ice model.

PERIDYNAMIC THEORY

The peridynamic theory was first introduced by Silling (2000) using an integral equation as a reformulation of the interactions between material points. A concept of a horizon is introduced, in which the material points interact through bonds, whereas the interactions disappear outside the horizon. For bond-based peridynamic theory, the governing equation of a material point at position $\mathbf{x}$ in the reference configuration can be written as

$$\rho(\mathbf{x})\ddot{\mathbf{u}}(\mathbf{x},t) = \int_{H_{\mathbf{x}}} \mathbf{f}(\mathbf{u}(\mathbf{x}',t) - \mathbf{u}(\mathbf{x},t), \mathbf{x}' - \mathbf{x}) dV_{\mathbf{x}'} + \mathbf{b}(\mathbf{x},t) \quad (1)$$

where ρ is the mass density of the reference configuration, $\mathbf{u}$ represents the displacement vector field, $\mathbf{b}$ is the body force, and $\mathbf{f}$ represents the pairwise force function showing the force per volume squared that the particle $\mathbf{x}'$ exerts on particle $\mathbf{x}$. $H_{\mathbf{X}}$ is the spherical neighborhood of referred radius δ centered at particle $\mathbf{x}$, called horizon. The relative position vector in the reference configuration is denoted by $\boldsymbol{\xi} = \mathbf{x}' - \mathbf{x}$ and the relative displacement vector at time t

is defined as $\boldsymbol{\eta} = \mathbf{u}(\mathbf{x}', t) - \mathbf{u}(\mathbf{x}, t)$.

The peridynamic forces between two particles interacting with each other are equal in magnitude and in the opposite directions. These forces are along the direction of the relative position vector in the current configuration and can be expressed as

$$\mathbf{f}(\boldsymbol{\eta}, \boldsymbol{\xi}) = f(\boldsymbol{\eta}, \boldsymbol{\xi}) \frac{\boldsymbol{\eta} + \boldsymbol{\xi}}{\|\boldsymbol{\eta} + \boldsymbol{\xi}\|} \tag{2}$$

As a microelastic material, the pairwise force function is derivable from the micropotential function $w(\boldsymbol{\eta}, \boldsymbol{\xi})$(Silling and Askari 2005) and can be written as

$$\mathbf{f}(\boldsymbol{\eta}, \boldsymbol{\xi}) = \frac{\partial w}{\partial \boldsymbol{\eta}}(\boldsymbol{\eta}, \boldsymbol{\xi}) \qquad \forall \boldsymbol{\eta}, \boldsymbol{\xi} \tag{3}$$

For a prototype microelastic brittle material proposed by Silling and Askari (2005), the pairwise force function is assumed to be linearly dependent on the deformation of the stretch between material points and can be defined as

$$\mathbf{f}(\boldsymbol{\eta}, \boldsymbol{\xi}) = c(\boldsymbol{\xi}) s(\boldsymbol{\eta}, \boldsymbol{\xi}) \frac{\boldsymbol{\eta} + \boldsymbol{\xi}}{\|\boldsymbol{\eta} + \boldsymbol{\xi}\|} \tag{4}$$

in which s is the stretch of the bond which can be expressed as

$$s(\boldsymbol{\eta}, \boldsymbol{\xi}) = \frac{\|\boldsymbol{\eta} + \boldsymbol{\xi}\| - \|\boldsymbol{\xi}\|}{\|\boldsymbol{\xi}\|} \tag{5}$$

and c represents the bond constant, analogous to the spring constant in Hooke's law. By equating the strain energy density of an individual material point from peridynamics with classical continuum mechanics, the bond constant c for a 2 Dimensional isotropic material can be written as

$$c(\boldsymbol{\xi}) = \frac{6E}{\pi \delta^3 b(1 - \nu)} \tag{6}$$

where E represents the elastic modulus of the material, b is the thickness of the plate, and ν is the Poisson's ratio which is limited to 1/3 in the bond-based peridynamic model.

ICE PROPERTIES

Ice is a complex material consisting of fresh water ice, gas, brine, and different types of solid salts, and shows dependence on the temperature. A single ice crystal behaves as a strong anisotropic material due to its dislocation glide on the basal plane, which is perpendicular to the crystal hexagonal symmetry axis, named as c-axis (Gagliardini, et al., 2009). During the time of the ice growth, environmentally dominated variations as well as the thermal and deformation history lead to the formation of different grain structures of ice. The most common grain structures include granular, columnar, and discontinuous columnar (Timco and Weeks, 2010). In this study, the freshwater columnar grained ice is considered. This type of ice is usually found in the lower layers of lakes and rivers. The ice is composed of columnar crystals which may elongate through the whole thickness of the level ice along the vertical direction. The c-axis of ice crystal are oriented randomly on the plane perpendicular to the direction of the columns. Thus, the columnar ice shows transversely isotropic material behaviour.

PERIDYNAMIC MICROMECHANICAL MODEL FOR ICE CRYSTALS

In this study, a microscopic material model is implemented to depict the behavior of the polycrystalline ice with random crystal orientations. In the polycrystalline structure, each grain is represented using bond-based peridynamics and introducing different bond properties along

the crystal orientation direction and other directions. Thus, the peridynamic bonds are divided into two types as shown in Figure 1. The type 1 bonds (shown with orange colour) exist in all the directions and describes the interaction between material points i and all other material points in the horizon, denoted by the peridynamic bond constant c_1. Type 2 bonds (shown with pink colour) only exist along the crystal orientation direction, θ. Therefore, the interaction of material points along the crystal orientation direction can be represented by the bond constant c_2. The peridynamic constitutive model for the in-plane interactions between two material points can be expressed using Equation (4) by assigning the relevant bond constant value depending on the bond orientation with respect to crystal orientation. According to Oterkus and Madenci (2012), by equating the strain energy densities of a material point based on classical continuum mechanics with bond-based peridynamics under simple loading conditions, the peridynamic material constants c_1 and c_2 can be expressed by the reduced stiffness matrix, Q_{ij} as

$$c_1 = \frac{24Q_{12}}{\pi b \delta^3} \tag{7}$$

$$c_2 = \frac{Q_{11} - Q_{22}}{\beta} \tag{8}$$

where

$$\beta = \frac{1}{2}\sum_{q=1}^{m} \xi_{qi} V_q \tag{9}$$

in which m represent the number of bonds along the crystal orientation direction within the horizon δ of material point i. ξ_{qi} is the initial length of the bond along the crystal orientation direction between material point q and i, V_q donates the volume of the material point q, and b is the thickness.

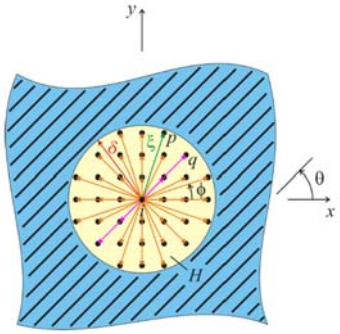

Figure 1. Horizon of a material point with a crystal orientation of θ

NUMERICAL RESULTS AND DISCUSSION

In this section, three static problems are considered by using bond-based peridynamic polycrystalline ice model described above. The numerical results are compared with the results obtained from FEM in order to verify the accuracy of the peridynamic polycrystalline ice model. For the polycrystalline ice simulations, the polycrystalline structure is generated by implementing the Voronoi tessellation method. The reduced stiffness matrix of a single grain can be written as

$$[Q] = \begin{bmatrix} Q_{11} & Q_{12} & 0 \\ Q_{12} & Q_{22} & 0 \\ 0 & 0 & Q_{66} \end{bmatrix} \quad (10)$$

According to Elvin (1996), the stiffness properties of a polycrystalline ice can be specified as $Q_{11} = 12.624\text{GPa}$ and $Q_{22} = 10.328\text{GPa}$.

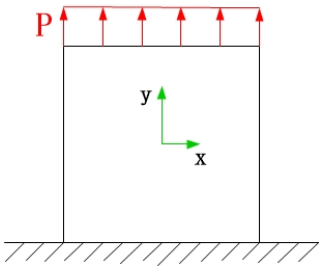

Figure 2. Single grain for static analysis

Single grain under uniaxial tension

The aim of this example is to show the accuracy of the elastic behaviour of the peridynamic columnar ice model. The crystal employed in this case has a length of 1.2 mm and a width of 1.2 mm. It is discretized uniformly with 200 particles distributed along the horizontal and vertical directions. Three layers of virtual particles are added along the bottom edge of the plate and set with zero displacements to constrain the bottom edge of the plate. A vertical load of $P = 600\text{MPa}$ is applied as a body force and exerted to the top edge of the plate as the boundary condition as shown in Figure 2. The quasi-static solution is obtained by implementing the adaptive dynamic relaxation method. A constant horizon radius of $\delta = 1.809 \times 10^{-5}\text{m}$ is used corresponding to 3.015 times of the grid spacing as suggested by Madenci and Oterkus (2014).

The comparison of the horizontal and vertical displacements between the numerical results obtained from peridynamic and FEM simulations for a single grain with a 45-degree crystal orientation is shown in Figure 3 and 4.

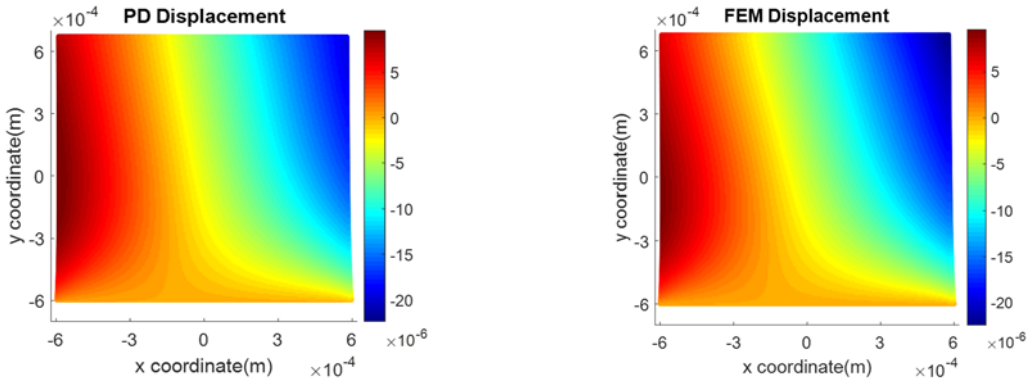

(a) Comparison of horizontal displacement field for single grain

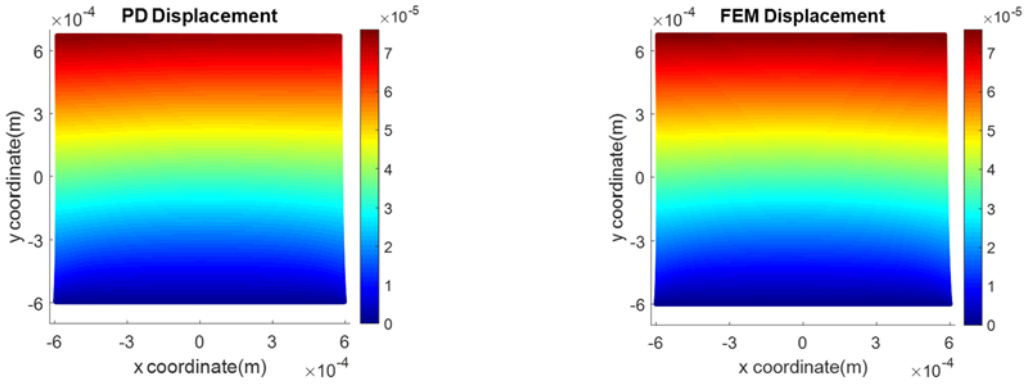

(b) Comparison of vertical displacement field for single grain

Figure 3. Comparison of displacement fields between PD and FEM for a single grain

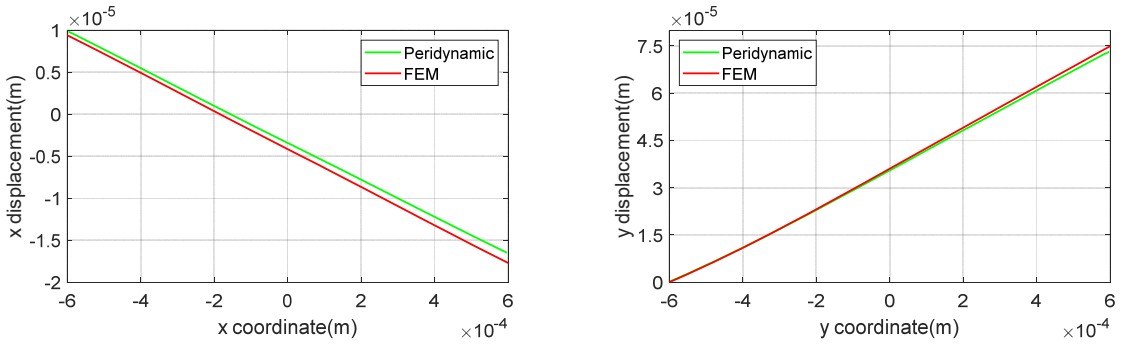

Figure 4. Comparison of horizontal and vertical displacements along the central axis between PD and FEM for a single grain

It is clear that the numerical results obtained from peridynamic simulation agree well with FEM results for a single ice grain under uniaxial tension loading. Therefore, the accuracy of the micromechanical peridynamic model for single grain is successfully verified.

Double grain model under uniaxial tension

In this section, double grain model with crystal orientations of -45 and 45 degrees are considered with a length of 2.4 mm and a width of 1.2 mm. The number of particles distributed uniformly along the horizontal and vertical directions is 300 and 150, respectively. The bottom edge of the plate is constrained with three layers of virtually added particles. The uniaxial tension loading of $P = 600\text{MPa}$ is applied as body force on the top edge of the plate. The horizon radius is defined as $\delta = 2.412 \times 10^{-5}$ m, i.e. 3.015 times of the grid spacing of $\Delta x = 0.008$ mm.

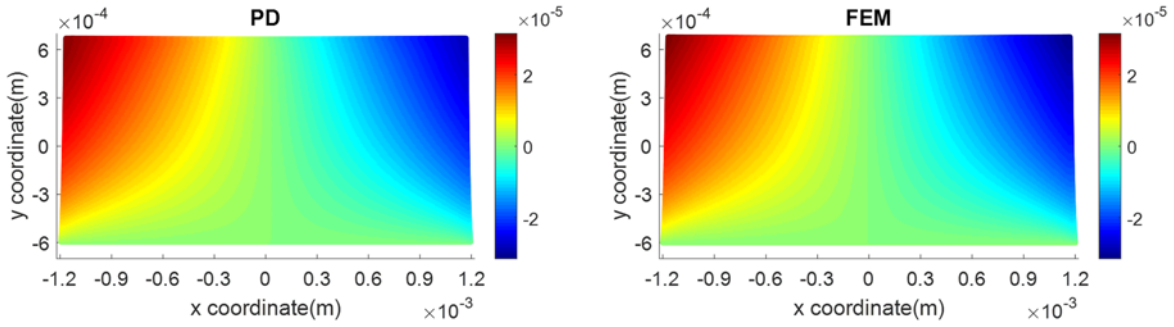

(a) Comparison of horizontal displacement field for double grain model

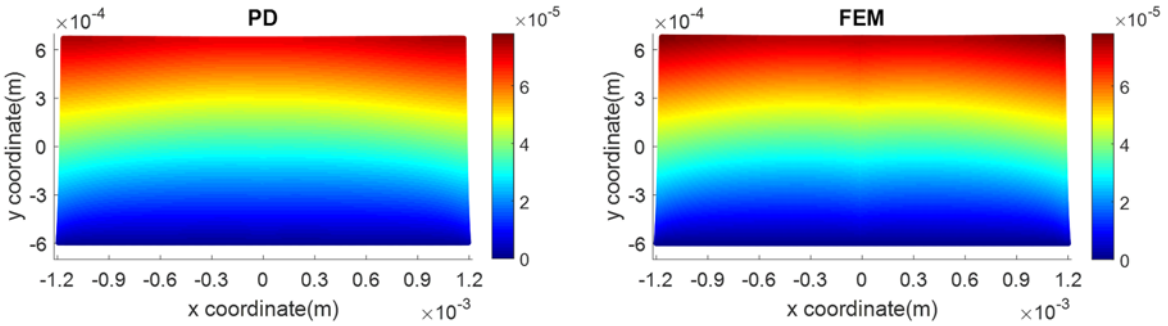

(b) Comparison of vertical displacement field for double grain model

Figure 5. Comparison of displacement fields between PD and FEM for double grain model

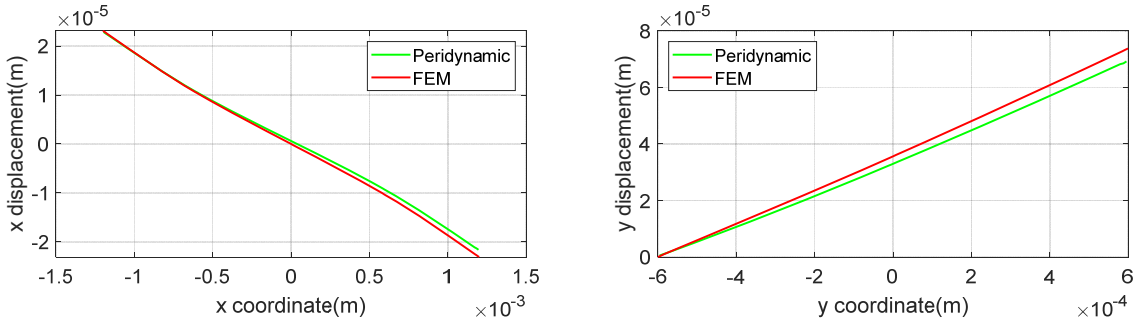

Figure 6. Comparison of horizontal and vertical displacements along the central axis between PD and FEM for double grain model

As depicted in Figure 5 and 6, the results obtained from peridynamic and FEM show good agreement in horizontal and vertical displacements for double grain model.

Static Analysis of polycrystalline ice

The polycrystalline ice modelled in this section consists of 100 randomly oriented grains (as shown in Figure 7) with the same ice properties used in the former examples. The plate has a length of 12 mm and a width of 12 mm. The domain is discretized with uniform grids with 200 particles distributed along the horizontal and vertical directions. Similar to the previous simulations three layers of virtual particles are set along the bottom edge of the plate to constrain the bottom edge. The top edge is subjected to a vertical load of $P = 600\text{MPa}$, applied as a body load through a volumetric region. The horizon radius is set as $\delta = 1.809 \times 10^{-4}$ m.

As shown in Figure 8 and 9, the numerical results based on the peridynamic theory match well with the results obtained from FEM. Only some small difference can be observed in the horizontal displacement field due to the approximate properties of the bonds between two different grains.

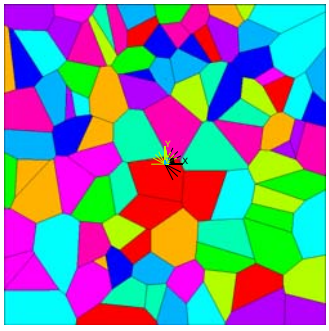

Figure 7. The distribution of grains in the polycrystalline ice considered for static analysis

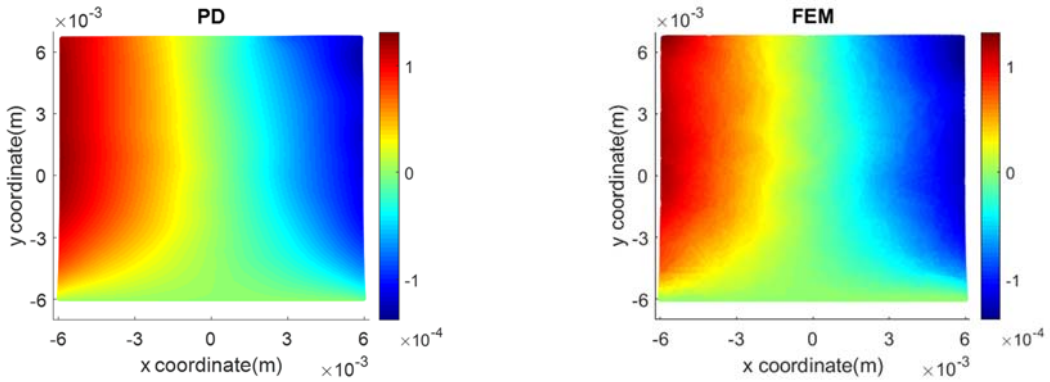

(a) Comparison of horizontal displacement field for polycrystalline ice

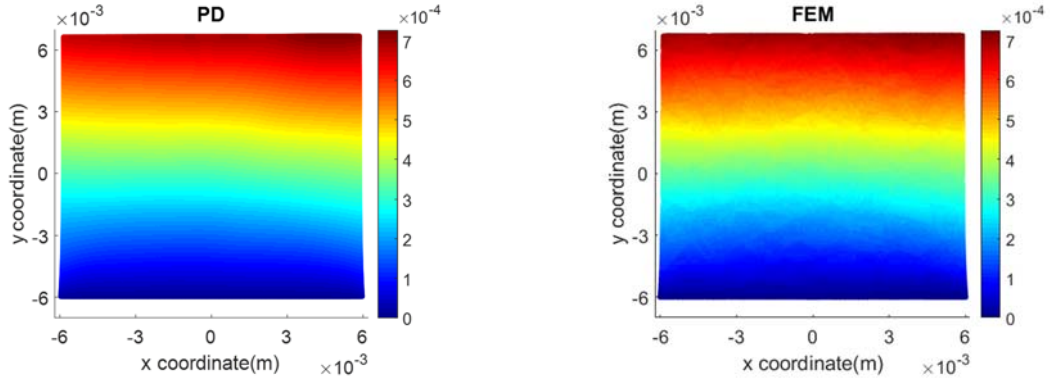

(b) Comparison of vertical displacement field for polycrystalline ice

Figure 8. Comparison of displacement field between PD and FEM for polycrystalline ice

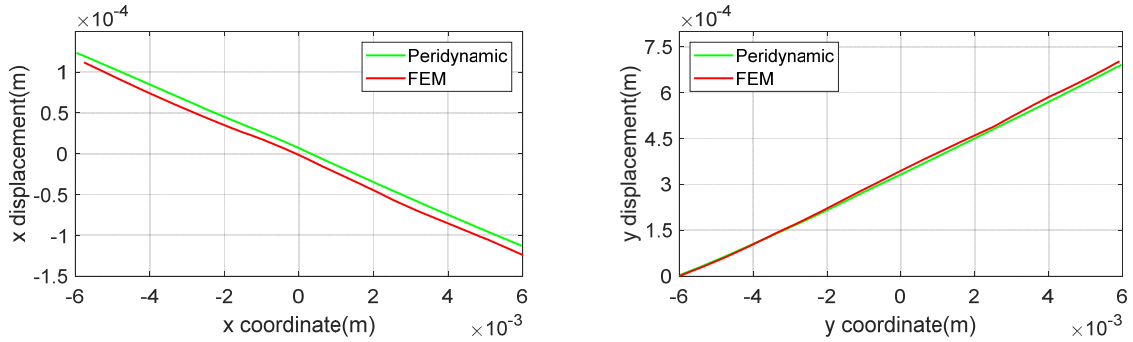

Figure 9. Comparison of horizontal and vertical displacement along the central axis between PD and FEM for polycrystalline ice

CONCLUSIONS

This paper presents a study of implementing the bond-based peridynamic theory, in which the equation of motion is an integral formulation rather than partial differential equation and is able to simulate the polycrystalline ice under uniaxial loading condition. In the simulations, freshwater columnar ice is considered as a transversely isotropic material. All grains in the ice are oriented randomly on the horizontal plane and modeled by using Voronoi tessellation method. The peridynamic parameters for the polycrystalline ice are calculated by equating the strain energy density of an individual material point based on classical continuum mechanics with peridynamics. The displacement fields along horizontal and vertical directions obtained from the numerical simulations are compared with the ones obtained from FEM, showing good agreement between peridynamic and FEM results. Thus, the accuracy of the peridynamic

polycrystalline ice model is successfully verified. Since the peridynamic theory has significant advantages in tackling problems with discontinuities, the fracture of polycrystalline ice will be modeled in a future study.

ACKNOWLEDGEMENTS

The authors gratefully acknowledges the financial support from China Scholarship Council (No. 201806680018) and University of Strathclyde.

REFERENCES

Askari, E., Bobaru, F., Lehoucq, R.B., Parks, M.L., Silling, S.A. and Weckner, O., 2008. Peridynamics for multiscale materials modeling. *In Journal of Physics: Conference Series* 125(1), p. 012078.

Crocker, A.G., Flewitt, P.E.J. and Smith, G.E., 2005. Computational modelling of fracture in polycrystalline materials. *International materials reviews*, 50(2), pp.99-125.

De Meo, D., Zhu, N. and Oterkus, E., 2016. Peridynamic modeling of granular fracture in polycrystalline materials. *Journal of Engineering Materials and Technology*, 138(4), p.041008.

Elvin, A.A., 1996. Number of grains required to homogenize elastic properties of polycrystalline ice. *Mechanics of Materials*, 22(1), pp.51-64.

Gagliardini, O., Gillet-Chaulet, F. and Montagnat, M., 2009. A review of anisotropic polar ice models: from crystal to ice-sheet flow models. *Physics of Ice Core Records*, 2, pp.149-166.

Gay, P., Hirsch, P.B. and Kelly, A., 1954. X-ray studies of polycrystalline metals deformed by rolling. III. The physical interpretation of the experimental results. *Acta Crystallographica*, 7(1), pp.41-49.

Ghajari, M., Iannucci, L. and Curtis, P., 2014. A peridynamic material model for the analysis of dynamic crack propagation in orthotropic media. *Computer Methods in Applied Mechanics and Engineering*, 276, pp.431-452.

Gold, L.W., 1960. The cracking activity in ice during creep. *Canadian Journal of Physics*, *38*(9), pp.1137-1148.

Gold, L.W., 1967. Time to formation of first cracks in ice. Physics of Snow and Ice. *Proceedings of the International Conference on Low Temperature Science*, pp.359-370.

Gold, L.W., 1999. Statistical characteristics for the strain-dependent density and the spatial position for deformation-induced cracks in columnar-grain ice. *Journal of Glaciology*, 45(150), pp.264-272.

Gribanov, I., Taylor, R. and Sarracino, R., 2018, October. Application of cohesive zone model to the fracture process of freshwater polycrystalline ice under flexural loading. *In IOP Conference Series: Earth and Environmental Science,* 1(1), p. 012013.

Liu, F., Baker, I., Yao, G. and Dudley, M., 1992. Dislocations and grain boundaries in polycrystalline ice: a preliminary study by synchrotron X-ray topography. *Journal of materials science*, 27(10), pp.2719-2725.

Madenci, E. and Oterkus, E., 2014. *Peridynamic theory and its applications*. New York: Springer.

Oterkus, E. and Madenci, E., 2012. Peridynamic analysis of fiber-reinforced composite materials. *Journal of Mechanics of Materials and Structures*, 7(1), pp.45-84.

Sfantos, G.K. and Aliabadi, M.H., 2007. A boundary cohesive grain element formulation for modelling intergranular microfracture in polycrystalline brittle materials. *International journal for numerical methods in engineering*, 69(8), pp.1590-1626.

Silling, S.A., 2000. Reformulation of elasticity theory for discontinuities and long-range forces. *Journal of the Mechanics and Physics of Solids*, 48(1), pp.175-209.

Silling, S.A. and Askari, E., 2005. A meshfree method based on the peridynamic model of solid mechanics. *Computers & structures*, 83(17-18), pp.1526-1535.

Sukumar, N., Srolovitz, D.J., Baker, T.J. and Prévost, J.H., 2003. Brittle fracture in polycrystalline microstructures with the extended finite element method. *International Journal for Numerical Methods in Engineering,* 56(14), pp.2015-2037.

Timco, G.W. and Weeks, W.F., 2010. A review of the engineering properties of sea ice. *Cold regions science and technology*, 60(2), pp.107-129.

Warner, D.H. and Molinari, J.F., 2006. Micromechanical finite element modeling of compressive fracture in confined alumina ceramic. *Acta Materialia*, 54(19), pp.5135-5145.